Activation detection in fNIRS by wavelet coherence

Xin Zhang[1], Haijing Niu[2], Yan Song[2], Yong Fan[1,*]
[1]National Laboratory of Pattern Recognition, Institute of Automation,
Chinese Academy of Sciences, Beijing 100190, China
[2]State Key Laboratory of Cognitive Neuroscience and Learning,
Beijing Normal University, Beijing 100875, China

ABSTRACT

Functional near infrared spectroscopy (fNIRS) is an optical technique measuring hemoglobin oxygenation and deoxygenation concentrations of the brain cortex with higher temporal resolution than current alternative techniques. The high temporal resolution enables collecting abundant brain functional information. However, the information collected by fNIRS is correlated and mixed with a variety of physiological signals. Due to the mixture effect, activation detection is one of challenges in fNIRS based studies of the brain functional activities. To achieve a better detection of activated brain regions from the complicated information measures, we present a multi-scale analysis method based on a wavelet coherence measure. In particular, the paradigm of an experiment is used as the reference signal. The coherence of the signal with data measured by fNIRS at each channel is calculated and summed up to evaluate the activation level. Experiments on simulated and real data have demonstrated that the proposed method is efficient and effective to detect activated brain regions covered by the fNIRS probe.

Keywords: fNIRS, activation detection, wavelet coherence, wavelet transform

1. INTRODUCTION

Functional near infrared spectroscopy has emerged as a low-cost and non-invasive technique to quantify brain functional activities[1, 2]. The mechanism of the technique is to emit near infrared light on subject's scalp and then detect scatted and diffused light on the scalp in the neighborhood of the source optode. The degree of attenuation of the light is closely related with changes in oxy-hemoglobin and deoxy-hemoglobin concentration in biomedical tissue[3]. Interpretation of fNIRS data relies on the neurovascular coupling in which neural activities are accompanied by locally increased metabolic demand and activated hemodynamics of cerebral tissue. Therefore, the *in vivo* measurements of fNIRS can reflect neurophysiological activity indirectly. Nowadays, studies of fNIRS have brought many improvements in the technique and ranged over applications concerning a variety of diseases, such as Alzheimer and schizophrenia[4]. The advantage of high temporal resolution in fNIRS is particularly critical in event-related studies, compared with alternative functional modalities.

The high temporal resolution of fNIRS enables collecting abundant physiological information of a subject. However, the physiological information is not organized in certain order, but mixed instead in a complicated way. The known sources of these physiological signals include cardic pulsation, respiration[5] and mean arterial blood pressure variations[6]. Moreover, most kinds of physiological signals are periodic and easily correlated between each other. In order to investigate a desired brain function by fNIRS, it is needed to separate the interested from others. Due to the difficulty of the separation, activation detection is one of the challenges in fNIRS although it is a necessary step to analyze brain functions. Therefore, the present paper explores a method of detecting brain activated areas, i.e., recovering brain areas which are on duty under certain task.

In fNIRS, the activation detection was solved by two methods hitherto. The first method adopted the general linear model (GLM), a model-driven method, in which various known regressors are involved to represent distinct physiological signals. Take an example, polynomial basis functions describe the instrumental and physiological drifts and Fourier basis functions reflect periodic signals. Then a regression method was used to keep the remaining error approaching Gaussian noise and accomplish an optimized estimation of parameters of regressors. The parameter of the regressor representing the task paradigm was evaluated against a threshold to indicate activated channels. The second

* yfan@nlpr.ia.ac.cn

Medical Imaging 2012: Biomedical Applications in Molecular, Structural, and Functional Imaging, edited by
Robert C. Molthen, John B. Weaver, Proc. of SPIE Vol. 8317, 831712 · © 2012 SPIE · CCC code: 1605-7422/12/$18
doi: 10.1117/12.911312

method estimates the hemodynamic response function (HRF) at each channel at first. Then a deviation index was used to illustrate activated channels. The GLM method was good at easy implementation, but it took the estimation in a linear and single scale model and the remaining error is hardly to resemble a Gaussian noise in practice. HRF-based method was also difficult to use, because the estimation of HRF is still a tough problem in fNIRS.

In the paper, we will present an activation detection method based on the wavelet coherence. It calculates the wavelet coherence between the experimental response and measured concentrations during a task in the time-frequency domain. The coherence is analyzed in the two domains and multiple scales, instead of in a single domain and single scale, like in GLM method. The experimental response is simulated by a convolution of stimuli with the canonical HRF. As the coherence is a local measure of correlation between two signals, the time-frequency coherence between the response and the concentrations reflects the local correlation with difference resolution. Therefore it can be used to detect local activation in a channel. The method avoids the selection of regressors in GLM method and calculation of HRF. Its performance has also been demonstrated by experiments in the third section of the paper.

This paper is structured as follows. In Section 2, we present the method of brain activation detection. Sections 3 describes experiments and investigates results to demonstrate the performance of the method. Section 4 concludes the work.

2. METHODS

2.1 Wavelet transform

A wavelet is a function with zero mean. It is characterized by a localization in both frequency ($\Delta\omega$) and time (Δt) domain, while Fourier basis is localized merely in the frequency domain. A simultaneous localizations in spatio-temporal domain plays a key role in a signal analysis so the localization can evaluate a wavelet function. According to the Heisenberg uncertainty principle, there always exists a tradeoff between localizations in the two domains. If there does not exist an appropriate balance between $\Delta\omega$ and Δt, a function would fail to achieve the minimum of the uncertainty product, $\Delta\omega \cdot \Delta t$ and then the function cannot analyze details of a signal in either domain. Wavelets proposed has been studied to reduce the product. So wavelet transform is employed here to analyze signals from fNIRS. One of wavelets is the Morlet wavelet, including a plane wave modulated by a Gaussian function,

$$\psi_0(\mu) = \pi^{(-1/4)} e^{(j\omega_0\mu)} e^{(-\frac{1}{2}\mu^2)}, \tag{1}$$

where ω_0 is dimensionless frequency and μ is the dimensionless time.

The wavelet transform is to decompose a signal in the time-frequency domain based on the wavelets. Due to the dual localization, a wavelet can divide a given function or signal into different scale components. In the transform, a wavelet is stretched in time by adjusting its scale (s), so that $\mu = s \cdot t$ and normalized it to have unit energy. Hence the transform has the advantage of high frequency resolution at low frequency parts and high time resolution at high frequency parts. It was defined that the wavelet transform of a time series ($x_n, n = 1, \ldots, N$) with uniform time steps δt is the convolution of x_n with the scaled and normalized wavelet,

$$\mathrm{W}_{x_n}(n,s) = \sqrt{\frac{\delta t}{s}} \sum_{n'=1}^{N} x_{n'} \psi_0 \left[(n'-n) \frac{\delta t}{s} \right]. \tag{2}$$

Accordingly, the wavelet power is defined as $|\mathrm{W}_{x_n}(s)|^2$.

2.2 Wavelet coherence

Given two time series x_n and y_n with wavelet transforms $\mathrm{W}_{x_n}(s)$ and $\mathrm{W}_{y_n}(s)$, the cross wavelet coherence is defined as $\mathrm{W}_{x_n,y_n} = \mathrm{W}_{x_n} \mathrm{W}_{y_n}^*$, where * denotes the complex conjugation. It recognizes regions in time frequency domain where the two signals co-vary. In the same manner, the wavelet power will be $|\mathrm{W}_{x_n,y_n}|$. Torrence and Webster defined the wavelet coherence of two time series as [7]

$$R^2(n,s) = \frac{\left|S\left(s^{-1}\mathrm{W}_{x_n,y_n}(n,s)\right)\right|^2}{S\left(s^{-1}\left|\mathrm{W}_{x_n}(n,s)\right|^2\right)\cdot S\left(s^{-1}\left|\mathrm{W}_{y_n}(n,s)\right|^2\right)}, \tag{3}$$

where S is a smoothing operator. The coherence is an extension to Pearson's correlation coefficient. The difference from the correlation resists in the fact that the coherence is time-locked and evaluate the correlation between two signals as a function of frequency[8]. A wavelet coherence tool box has been developed by Grinsted *et al.* on the MATLAB platform to do the wavelet transform and coherence analysis (http://www.pol.ac.uk/home/research/waveletcoherence/).

2.3 Confidence level

Wavelet coherence analysis provides the coherency between two signals, but the quantity is normalized between 0 and 1. There is an additional requirement of a metric assessing the coherence against that between two random signals, i.e., white Gaussian noise in our case. A confidence level is a good metric to illustrate that the coherence detected by Eq. 3 exists significantly.

In order to determine the confidence level of wavelet spectrum, the first step is to select an appropriate background spectrum and then the wavelet spectrum of a signal is to compare against the background one[9]. Matteau-Pelletier studied noise in fNIRS and proved that it was a pink noise (a.k.a., 1/f noise), i.e., power increased with frequency decreased proportionally[6]. Kaulakys analyzed that the noise can be generated by an autoregressive model[10]. Parameters of the model can be estimated from the signal.

Referring to the theory in the Fourier analysis, the normalized Fourier power spectrum is given by

$$E_k = \frac{N\left|X_k\right|^2}{2\sigma^2}, \tag{4}$$

where X_k represents Fourier transform results, N is the number of points and σ^2 is the variance of the signal. Without loss of generality, suppose the background noise is a white noise. Then $\left|X_k\right|^2$ is in a chi-square distribution with 2 degree of freedoms (DOFs). Because the wavelet transform can obtain from the inverse Fourier transform of the product, X_k and Ψ_k (Ψ_k is the Fourier transform of a wavelet function), $\left|\mathrm{W}_{x_n}(n,s)\right|^2$ is also in a chi-square distribution with 2 DOFs. Therefore, the distribution for the local wavelet power spectrum of a signal is

$$\frac{\left|\mathrm{W}_{x_n}(n,s)\right|^2}{\sigma^2} \Rightarrow \frac{1}{2} P_k \chi_2^2, \tag{5}$$

at each time n and scale s. Here σ^2 is the variance of the signal, χ_2^2 denotes a chi-square distribution with 2 DOFs and P_k is the mean spectrum at the wavelet scale s. Once a background spectrum is chosen, the 95% confidence level for χ^2 can be calculated by Eq. 5 and then the 95% confidence contour lines can be drawn by comparing the local wavelet power spectrum against $P_k\chi_2^2/2$. The contour can be used to recognize the region where the wavelet transform of the brain activation locate.

2.4 Activation detection by wavelet coherence

The fNIRS measures the hemoglobin oxygenation and de-oxygenation concentrations, which provide functional information of brain underlying certain motor or cognitive tasks. Hence the concentration should reflect the correlation between brain neurophysiology and behavioral tasks. The correlation has also been confirmed by functional magnetic resonance imaging and fNIRS[11]. In our case, the time-locked correlation, i.e., coherence in the region illustrated by 95% confidence contour, is used to evaluate the activated power of each channel against the task paradigm. If a channel is activated during a task, there are more changes of hemoglobin oxygenation and de-oxygenation according to the neurovascular coupling and vice versa. Therefore, the coherence with the confidence level is employed to detect an activated channel.

3. EXPERIMENT

There are two experiments conducted to demonstrate the performance of the activation detection method. In the first experiment, we adopts simulated data to verify that the activated channel is detected correctly. In the second experiment, data of doing visual stimuli is detected to present the activation area.

3.1 Experiment on simulated data

An experiment on simulated data can evaluate the accuracy of the detection method. The simulated data includes 22 channels. The data was measured during a resting state for 3000 seconds. In order to simulate an activated channel, we design a response by the convolution of canonical HRF with a set of stimuli. The stimuli start at 50 second and stay "on" for 10 seconds and "off" for 10 seconds. There are ten stimuli in the data. Then we contaminate the response with Gaussian White noise to remain the signal-to-noise ratio to 20dB.

The expected response is shown in Fig. 1, in which (a) is in the time domain and (b) is in the time-frequency domain after a wavelet transform. The color map in Fig. 1b is consistent with the confidence level. As these stimuli go at 0.05Hz, we can see a band circulated by a contour with black color at around 0.05Hz in Fig. 1b. The contour illustrates the region where the confidence level is over 95%. It means that the power in the region is more than that of physiological noise existing in fNIRS measurements significantly and the decomposition within the region should emerge from a desirable signal. So the region can be used as a mask to determine the power related with the task paradigm. The mask is shown in Fig. 2a.

The expected response is added into the measured resting-state data in the channels 6, 17 and 19 with the amplitude, 4×10^{-6}, 10×10^{-6} and 4×10^{-6}, respectively. The data of three channels plus channel 18 are shown in Fig. 3. Here channel 18 is shown as a reference without any response. The top four subfigures show simulated data in blue with corresponding response in red. They are in the same scale. Apparently, the response in channel 17 is more than those in other channels. The bottom four subfigures are wavelet coherence results of the four channels with expected response. Referring to these subfigures, there are obvious coherence over 95% confidence level located at 0.05Hz, except in channel 18 and the time range of these coherence are almost the same as that in Fig. 1b. The reason that there is no coherence in channel 18 is that we did not add any expected response into the channel.

The response we added into the three channel 6, 17, and 19 are not in the same amplitude. However the coherence at 0.05Hz does not increase proportionally with the amplitude, as the coherence is more significant in channel 6 than those in other channels. It is owing to the fact that the signal of channel 17 in the resting state has much more noise. These noise obscure response in the channel. But even though, the method is still applicable to detect the coherence in the channel.

The coherence of each channel within the mask shown in Fig. 2a is summed up. The summation is an index to show the

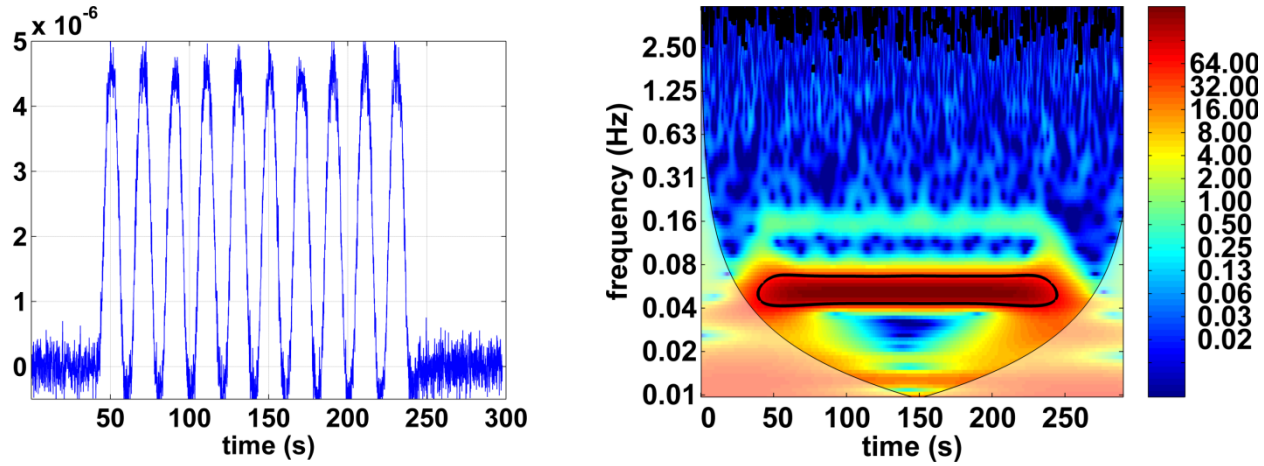

(a) Expected response

(b) Wavelet transform of expected response.

Fig. 1 Expected response is shown in (a) and its wavelet transform is shown in (b). The contour delineated by black line in (b) is drawn by the 95% confidence level.

activation level. The final map of activation levels of channels is drawn in Fig. 2b. In the subfigure, the red square indicates the position of every channel and numbers on the left side of these squares are the channel label. There is an obvious activation in channel 17. The activation map is consistent with the configuration of the experiment.

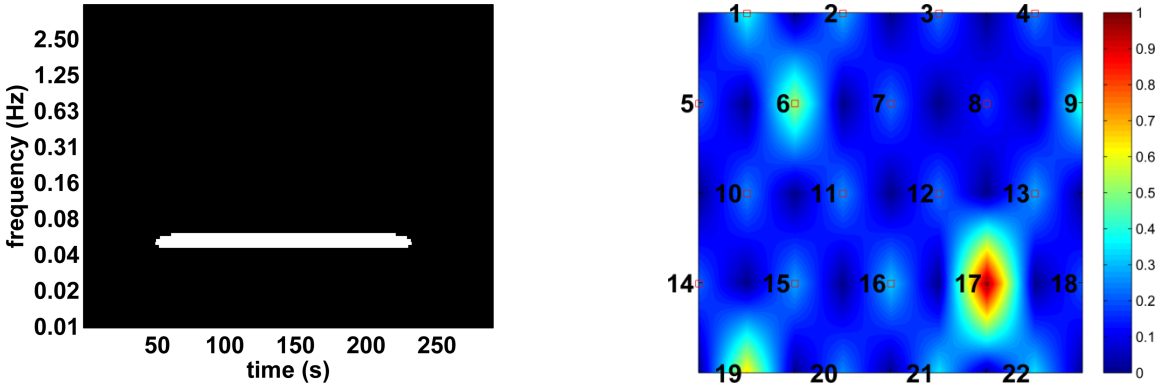

(a) (b)

Fig. 2 Mask shown in (a) is to determine the region related with task paradigm in time frequency domain; (b) is the activation map in the fNIRS probe.

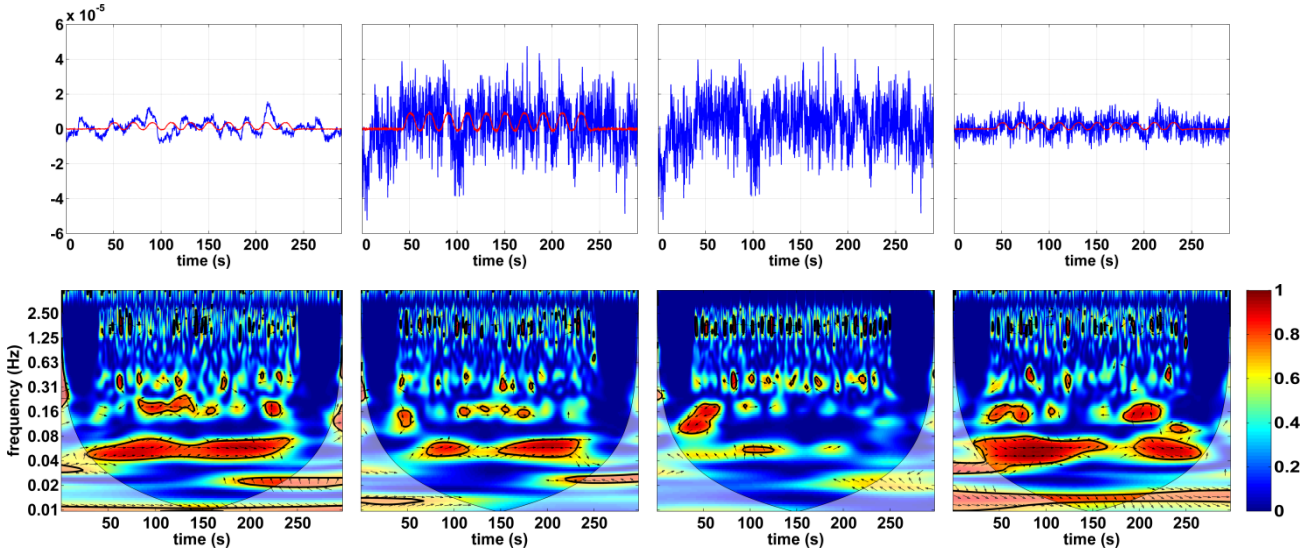

(a) Channel 6 (b) Channel 17 (c) Channel 18 (d) Channel 19

Fig. 3 Simulated data of the four channels, 6, 17, 18 and 19. The top four subfigures are in the time domain with data in blue and corresponding response in red. The bottom four subfigures are wavelet coherence results of the four channels with expected response. The results have been normalized into [0, 1].

3.2 Experiment on real data

An experiment on real data is necessary to testify the detection method. In the experiment, subjects conduct a visual stimulation task. In the beginning 120 seconds, subjects are staying quietly and data are measured in the resting state. From the 120s, subjects are exposed to the visual stimuli periodically. A trial includes a stimulus for 20 seconds and then a resting state for 20 seconds. So the frequency of the trail is at 0.025Hz. The stimuli paradigm is shown in Fig. 4a and its wavelet transform result is in Fig. 4b. The black contour delineates the significant region against noise. The region is set as a mask for following analysis, shown in Fig. 4c. The wavelet coherence analyzes the coherence between the experimental paradigm and each channel data. Two typical coherences are drawn in Fig. 5a and Fig. 5b. In Fig. 5a, there is not significant coherence, while in Fig. 5b, a significant region is obvious. Moreover, referring to the subfigure, the

region is located at the band of 0.025Hz, which corresponds to that of the experimental paradigm in Fig. 4b. The summation of power correlating with the experimental paradigm is used to indicate the level of activation in a channel. Then these levels are organized in the same position as optodes in the probe. The activation map is shown in Fig. 5c.

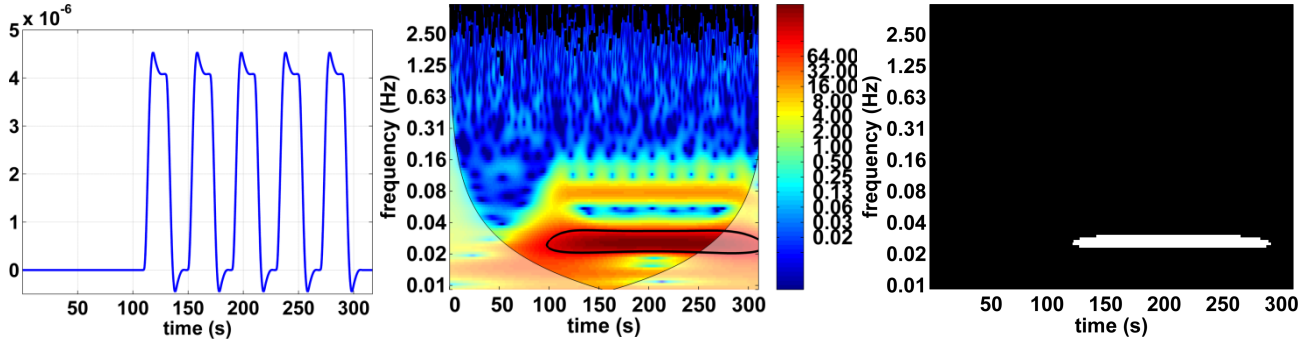

(a) Expected response (b) Wavelet transform of the response (c) Mask

Fig. 4 Expected response in the visual experiment is shown in (a); (b) is the wavelet transform of the response with 95% confidence contour in black and (c) is the mask delineated by the contour in (b).

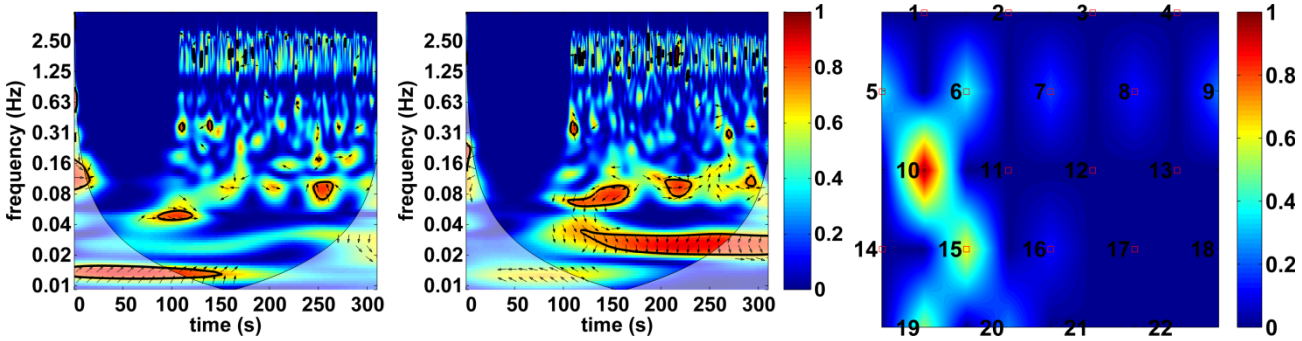

(a) Wavelet coherence of channel 1 (b) Wavelet coherence of channel 10 (c) Activation map

Fig. 5 Subfigures (a) and (b) show wavelet coherence of channel 1 and 10 and (c) presents the activation map.

4. CONCLUSIONS

The activation detection method makes use of the wavelet coherence to explore activated area, which is based on the wavelet transform decomposing a channel data into the time-frequency domain with multiple scales. The analysis tool separates the physiological noise from the interested signal in channel data effectively. Wavelet coherence correlates the data with the experimental paradigm time-locked, which works well to evaluate the correlation locally and indicates parts consistent with the paradigm. The most correlated part illustrates the level of activation in a channel. Two experiments on simulated and real data demonstrate that the coherence performs the detection correctly and effectively.

ACKNOWLEDGEMENTS

This work was partially supported by the Natural Science Foundation of China, Grant Nos. 81101082, 60831004.

REFERENCES

[1] Jobsis, F. F., "Noninvasive, infrared monitoring of cerebral and myocardial oxygen sufficiency and circulatory parameters," Science, 198(4323), 1264-7 (1977).

[2] Villringer, A., Planck J., Hock C. *et al.*, "Near infrared spectroscopy (NIRS): a new tool to study hemodynamic changes during activation of brain function in human adults," Neurosci Lett, 154(1-2), 101-4 (1993).

[3] Irani, F., Platek S. M., Bunce S. *et al.*, "Functional Near Infrared Spectroscopy (fNIRS): An Emerging Neuroimaging Technology with Important Applications for the Study of Brain Disorders," Clin Neurophysiol, 21(1), 9 - 37 (2007).

[4] Zhu, Y., Liu X., Wang H. *et al.*, "Reduced prefrontal activation during Tower of London in first-episode schizophrenia: a multi-channel near-infrared spectroscopy study," Neurosci Lett, 478(3), 136-40 (2010).

[5] Franceschini, M. A., Gratton E., and Fantini S., "Noninvasive optical method of measuring tissue and arterial saturation: an application to absolute pulse oximetry of the brain," Opt. Lett., 24(12), 829-831 (1999).

[6] Matteau-Pelletier, C., Dehaes M., Lesage F. *et al.*, "1/f Noise in Diffuse Optical Imaging and Wavelet-Based Response Estimation," IEEE Transactions on Medical Imaging, 28(3), 415-422 (2009).

[7] Torrence, C., and Webster P. J., "Interdecadal changes in the {ENSO-Monsoon System}," J. Clim., 12, 2679-2690 (1999).

[8] Caviness, J. N., Adler C. H., Sabbagh M. N. *et al.*, "Abnormal corticomuscular coherence is associated with the small amplitude cortical myoclonus in Parkinson's disease," Movement Disorders, 18(10), 1157-1162 (2003).

[9] Torrence, C., and Compo G. P., "A practical guide to wavelet analysis," Bulletin of the American Meteorological Society, 79(1), 61-78 (1998).

[10] Kaulakys, B., "Autoregressive model of 1/f noise," Physics Letters A, 257(1-2), 37-42 (1999).

[11] Huppert, T. J., Hoge R. D., Diamond S. G. *et al.*, "A temporal comparison of BOLD, ASL, and NIRS hemodynamic responses to motor stimuli in adult humans," NeuroImage, 29(2), 368-82 (2006).